Abstract:

Multi-carrier energy systems have received wide currency by improving cogeneration facilities. Although these systems show significant efficiency in providing and consuming energy, the performance of the whole system can be reduced owing to uncertainties arising from different sources. This paper presents a stochastic decentralized model for considering the uncertainties of a system including different types of thermal and electrical private loads using a multi-agent framework. In other words, agents have private ownership and seek for social welfare as well as the personal profits optimization. In the proposed model, the gradient projection method is used to implement a fully-decentralize energy trading model. Also, various stochastic scenarios of solar irradiance, prices, and loads are considered using fast-forward selection algorithm to take into account the uncertainties. Then, to assess the proposed stochastic multi-agent model, "AnyLogic" is used for simulation. The numerical results show that the clearing price is directly affected by the renewable agent without any supervisory control. Moreover, the total operating cost of the considered multi-carrier energy system decreases by ~7% considering these uncertainties compared with deterministic one. However, social welfare declines due to the intrinsically beneficial behavior in private cooperation.

Keywords:

Renewable energy– Decentralized operation – Stochastic optimization – Multi-agent systems, Uncertainty.

Nomenclature

Indices	Parameters
i $\quad First\ type\ of\ generator$	$\eta_{ch}^{es}/\eta_{dich}^{es}$ $\quad charging/discharging\ efficiency$
j $\quad Second\ type\ of\ generator$	$p_{ch}^{esMax}/p_{disch}^{esMax}$ $Max\ power\ of\ \ charging$ $/discharging$
k $\quad First\ type\ of\ consumer$	it $\quad number\ of\ iterations$
l $\quad Second\ type\ of\ consumer$	soc_{min}^{bat} $\quad Minimum\ state\ of\ charge\ of\ battery$
t $\quad Time$	n_s $\quad Number\ of\ stochastic\ scenarios$
$(.)_s$ $\quad In\ scenario\ s$	α/β $\quad Beta\ distribution\ parameters$
Decision variables	
$\lambda_s(t)$ $\quad Settlement\ price$	**Abbreviations**
$p_{mt,s}^{e}(t)$ $\quad Electric\ power\ of\ micriturbine$	EH Energy hub
$p_{mt,s}^{h}(t)$ $\quad Heat\ power\ of\ microturbine$	FTOG First type of generator
$p_{dis,s}^{es}(t)$ $\quad Discharge\ power\ of\ battery\ \ storage$	FTOC First type of consumer
$p_{ch,s}^{es}(t)$ $\quad Charge\ power\ of\ battery\ storage$	MAS Multi-agent system
$\alpha_{dis\|ch,s}^{e}(t)$ $\quad Binary\ status\ of\ battery\ storage$	MT Micro-turbine
${soc_s}^{es}(t)$ $\quad State\ of\ charge\ of\ battery$	PV Photovoltaic
$p_{g1}(t)$ $\quad Power\ of\ first\ type\ of\ generators$ $(MT\ and\ boiler)$	PDF Probability distribution function
$p_{g2}(t)$ $\quad Power\ of\ second\ type\ of\ generators$ $(PV\ and\ main\ grid)$	STOG Second type of generator
$p_{d1}(t)$ $\quad Power\ of\ first\ type\ of\ consumers$ $(thermal\ and\ electrical\ loads)$	STOC Second type of consumer
$p_{d2}(t)$ $\quad Power\ of\ first\ type\ of\ consmers$ $(cooling\ load)$	VSS Value of a stochastic solution
p_{req}^{es} $\quad required\ power\ from\ battery$	
$P_{mth}^{min}(t)$ $\quad minimum\ heat\ production\ of\ MT$	

1. Introduction

1.1. Motivation

The development of decentralized systems has received more attention due to the inefficiency of centralized management systems in the presence of distributed generation resources as well as competitive market mechanisms [1, 2]. The development of these systems along with increasing the penetration of renewable resources could bring about the elimination of intermediaries, reducing environmental pollution, job creation, and reduction in the cost of network expansion in remote areas [3]. As a result, this could lead to the sustainable development of the energy systems through expanding of multi-carrier systems instead of single-carrier ones. Multi-carrier energy systems or energy hubs (EHs) include multiple energy conversion, storage, and/or network topologies [4]. They integrate multiple types of energy resources including renewable and traditional grids to meet the consumer's more efficiently. The EHs are managed for residential [5, 6] commercial [7] or energy use [8-11] by different management strategies, especially decentralized methods[12]. The flexibility of decentralized methods, Plug and Play feature and private ownership are some of their popular applications [13, 14].

On the other hand, the result of the operation can be affected by several uncertainties in the system [15-18]. There are two types of uncertainty for the operation of an EH. The first one is operational parameters which are related to operating decisions like electric, heat, and cooling loads or renewable generation. The second one is economic parameters like electric and gas prices [19]. Since these parameters are input data for agents' operation, the difference between the predicted values and the actual values will affect their decision making and personal profits. Therefore, it is necessary to develop a decentralized framework that can capture the uncertainties of renewables and the prices.

1.2. Literature survey

The decentralized operation of EHs has been considered in many research works. A multi-agent system (MAS) has been confirmed as an efficient approach for managing decentralized systems [3, 20, 21] and is used in [22-27] with different layers including switching control, dynamic control, and energy management. Although the computational burden is reduced in these works, there is still a dependency on the central agent. Also, the uncertainties are ignored. The proposed model in [28] based on the master-slave method only examines the impact of energy carrier on the operational decisions and the central agent's trouble is still ignored. Both thermal and electrical markets proposed in [29] aim at consumers' cost minimization but ignoring the agent's profit and operating uncertainty. The distribution system operator agent is also essential in [30, 31] as the central agent to control several EHs and micro-grids. The optimal performance of agents in [32] for a multi-carrier system is investigated using a reinforcement learning algorithm, but there is an energy manager in the upper level of the system to supervise the market and prices. Likewise, decentralization modeled in [33] using alternating direction method of multipliers (ADMM) is still dependent on the distribution system operator.

The social welfare of EHs is considered in [34] with the game theory which is used to omit the central agent, but the personal profits of agents are neglected. The need for a central agent is omitted using the Consensus Theorem algorithm, the Gradient projection method, and the Lagrange method in [35-37]. In [38], the interaction among EHs is considered by a game to optimize the payments of EHs. Also, in [39], the MAS is used for optimal energy management of micro-grid and robust optimization is used to consider renewable uncertainty. In all of these studies, social welfare is only considered for optimization without attention to agent's benefits despite considering a decentralized operation. Also, the models have not seen both the cost function of renewable agents and interaction with the upstream network as a second-order basis. Although this gap is filled in [40] and the renewable agent can independently act as a price-maker agent, the uncertainty of renewable generation is ignored. Similarly, the fully-decentralized framework is implemented for a multi-carrier system in [41] without any emphasis on the uncertain data. However, the robust optimization is used in [42] considers the renewable uncertainties of multiple micro-grids with decentralized management but the system is single-carrier yet.

There are some related works in [43-48] for the operation of EHs considering different uncertainty but in a centralized manner. In the same way, in [49], a hybrid robust-stochastic approach is used to deal with different uncertainties in a multi-carrier micro-grid with centralized management. Due to the increase in renewable penetration rate and therefore, data changes, the performance of the centralized model will be decreased [50].

Table 1. Comparison of relevant works

Reference	Centralized operation	Decentralized operation	Multi-carrier	Renewable unit	Private ownership	Uncertainty
[5, 29, 35]	×	✓	✓	✓	×	×
[6, 7, 9]	✓	×	✓	✓	×	×
[8]	×	✓	✓	✓	×	×
[10, 47]	×	✓	✓	✓	×	✓
[13, 26, 28]	×	✓	×	✓	×	×
[22, 23, 25, 48, 51]	✓	×	×	✓	×	×
[3, 30, 31]	✓	×	✓	✓	×	×

[32, 33]	×	✓	✓	×	×	×
[34]	×	✓	×	×	×	×
[37, 38]	×	✓	✓	×	×	✓
[39, 42]	×	✓	×	✓	×	✓
[40, 41]	×	✓	✓	✓	✓	×
[43-46, 49]	✓	×	✓	✓	×	✓

1.3. Contributions

Due to the previous works and Table 1, there is a need to design a decentralized optimization framework for a multi-caries energy system or EH in which the private profits for agents and the independent operation of each agent considering their uncertainties are involved. In this paper, the effect of uncertainties on the solutions is analyzed using stochastic scenarios. The renewable agent is a price-maker agent without dependency on any central control unit. This agent helps both power balance constraints and personal benefits using the storage system. Therefore, the contributions of this paper are:

- Proposing the active presence of a renewable agent in a fully-decentralized optimization framework.
- Modeling private ownership using a multi-agent framework.
- Considering uncertainties of operating parameters such as prices, solar irradiance, and loads and analyzing their effect on performance indicators of the system's operation.

The remainder of this paper is organized as follows. The proposed EH model will be explained in Section 2. The stochastic scenarios formation and the decentralized operation model will be given in Section 3 and Section 4, respectively. Also, the simulation and conclusion will be presented in Sections 5 and Section 6, respectively.

2. System description

An overview of EH with its agents is shown in Fig. 1. These agents include photovoltaic (PV), boiler, micro-turbine, grid, cooling, thermal, and electrical loads. These agents with private ownership communicate with each other to maximize social welfare. In this model PV agent includes battery storage and solar units. In this EH, the battery storage and upstream grid are used for balancing the electrical power. To clarify the exact framework of the proposed model, the following assumptions are considered:

- Various agents own the elements of their subset.
- The capacity to exchange electrical power with the upstream grid is limited.
- The price of buying and selling electricity inside the EH is determined on an hourly basis based on the intended interactions.
- The EH does not have a thermal or cooling exchange with the upstream network.
- The solar factor is the only factor that can sell electricity to the upstream network separately.

To cover the presence of renewable energy, the PV agent has been considered. For applying the demand response, both electric and thermal loads have contractions concerning price variation. The reason for the presence of MT is having a connection between the two heating and electrical networks. To have a multi-energy system, the cooling load is also placed as a participant in the electrical and thermal network. The battery storage is taken into account as a control unit against the intended uncertainties.

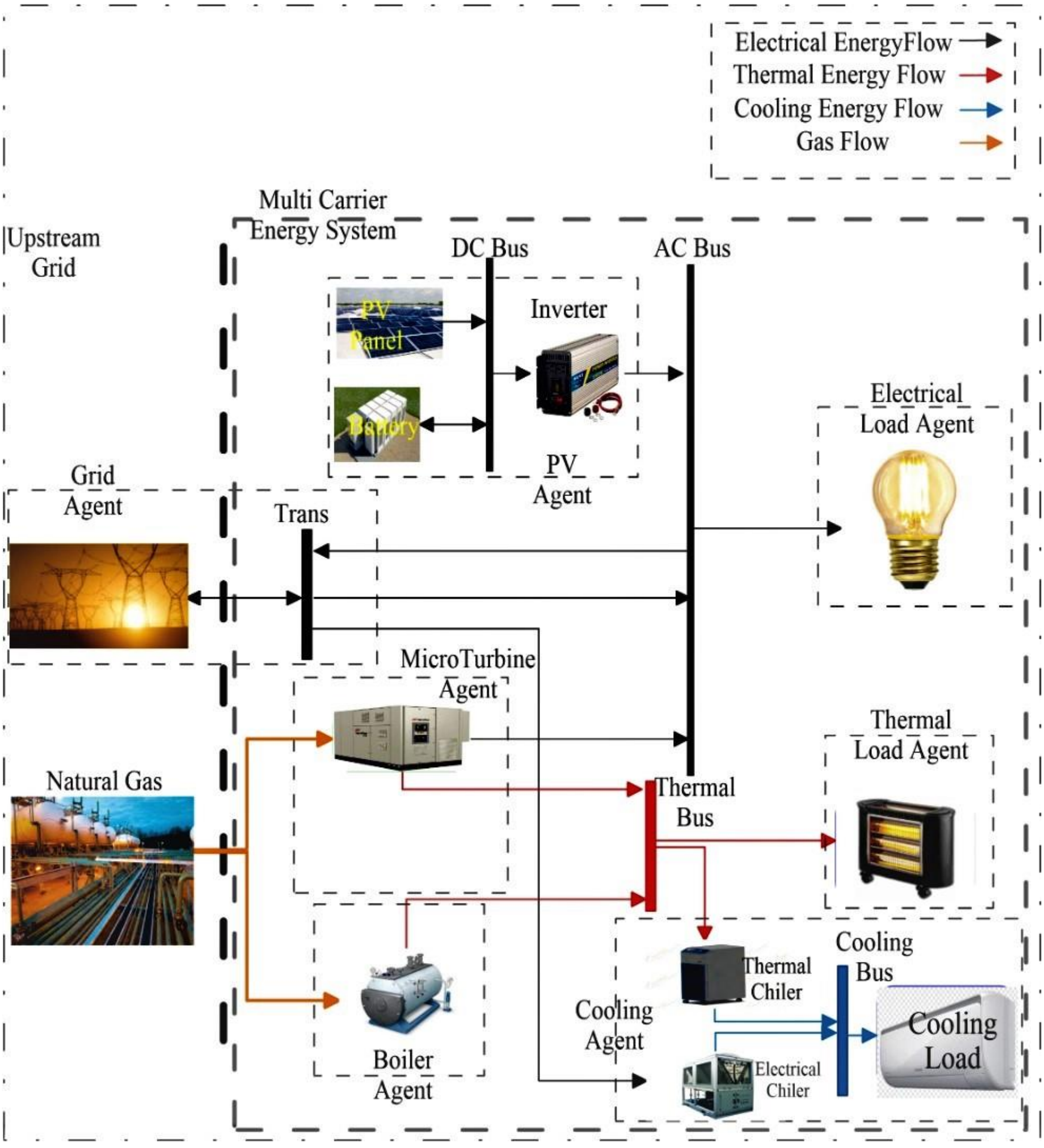

Fig. 1. EH model

3. Decentralized model for operation

In this section, first, the type of agents is described, and then the social welfare function is constructed for the deterministic problem. Finally, the gradient projection algorithm is explained for decentralization. There are four types of agents in this model in which two of them are generators and the others are the consumers. Moreover, the generators and consumers are sellers and buyers respectively. It is worth to mention that, all formulation is valid for both electrical and thermal cooperation. So, it is a general form of formulation for both electrical and thermal settlement prices.

3.1. First type of generators (FTOGs)

The operational cost function of the FTOGs like Boiler and MT agents is as Eq. (1). a_{g1}, b_{g1} and c_{g1} are positive cost coefficients and $p_{g1}(t)$ is the output power of the FTOGs at time *t*. Also, the generators' income at time *t* is modeled in (2) where $p_{g1}(t)$ is their generated power at time *t* and $\lambda(t)$ is the settlement price [52].

$$C_{g1}(t) = \frac{1}{2} a_{g1} * p_{g1}(t)^2 + b_{g1} * p_{g1}(t) + c_{g1} \tag{1}$$

$$R_{g1}(t) = \lambda(t) * p_{g1}(t) \tag{2}$$

3.2. Second type of generators (STOGs)

The cost function for this kind of generators (PV and grid agent) is defined by Eq. (3) where c_{g2} is their constant cost. Also, the generators' income at time *t* is modeled in (4) where $p_{g2}(t)$ is their generated power at time *t* and $\lambda(t)$ is the settlement price [52].

$$C_{g2}(t) = c_{g2} \tag{3}$$

$$R_{g2}(t) = \lambda(t) * p_{g2}(t) \tag{4}$$

3.3. Types of consumer

The benefit function for the loads of first type of consumers (FTOCs) such as thermal and electrical loads is modeled as (5). a_{d1} and b_{d1} are cost function for the FTOCs where the former is negative and the latter is positive. Also, $p_{d1}(\mathrm{t})$ is the demand power at time *t* and its cost function is modeled as (6) [52].

$$R_{d1}(t) = \frac{1}{2}a_{d1} * p_{d1}(t)^2 + b_{d1} * p_{d1}(t) \tag{5}$$

$$C_{d1}(t) = \lambda(t) * p_{d1}(t) \tag{6}$$

Regarding the second type of consumers (STOCs) which is the cooling agent as is depicted in Fig. 1, the strategy is the selection of lower price between thermal and electrical interactions to minimize its own cost in Eq. (6). $p_{d2}(\mathrm{t})$ is the cooling demand at time *t* [52]. This agent has not benefit functions because it always purchases demand.

$$C_{d2}(t) = \lambda(t) * p_{d2}(t) \tag{7}$$

3.4. Social welfare function

The social welfare function of this EH is defined as (8) and consists of incomes of agents minus their costs. n_{d1} and n_{d2} are the numbers of FTOCs and STOCs. Also, n_{g1} and n_{g2} are the numbers of FTOGs and STOGs.

$$SWF = \sum_{t=1}^{24}\left(\sum_{i=1}^{n_{g1}}(R_{g1}^{i}(t) - C_{g1}^{i}(t)) + \sum_{j=1}^{n_{g2}}(R_{g2}^{j}(t) - C_{g2}^{j}(t)) + \sum_{k=1}^{n_{d1}}(R_{d1}^{k}(t) - C_{d1}^{k}(t)) - \sum_{l=1}^{n_{d2}} C_{d}^{l}(t)\right) \tag{8}$$

Plugging Eqs. (1) – (7) into (8) results in (9) as presented below:

$$SWF = \sum_{t=1}^{24}\left(\sum_{k=1}^{n_{d1}}(\frac{1}{2}a_{d1}^{k} * p_{d1}^{k}(t)^2 + b_{d1}^{k} * p_{d1}^{k}(t)) - \sum_{i=1}^{n_{g1}}\left(\frac{1}{2}a_{g1}^{i} * p_{g1}^{i}(t)^2 + b_{g1}^{i} * p_{g1}^{i}(t) + c_{g1}^{i}\right) - C_{g2}n_{g2} + \lambda(t) * (\sum_{i=1}^{n_{g1}} p_{g1}^{i}(t) + \sum_{j=1}^{n_{g2}} p_{g2}^{j}(t) - \sum_{k=1}^{n_{d1}} p_{d1}^{k}(t) - \sum_{l=1}^{n_{d2}} p_{d2}^{l}(t))\right) \quad (9)$$

Existing parameters can be updated using the gradient projection algorithm to maximize objective function (9) [53]. Explaining the basis of this algorithm is beyond the scope of this paper. The distributed variables are written in Eqs. (10) -(14). In these equations, ε^{it} is the step size of this algorithm and the higher value for this parameter, the higher speed we will have for reaching the answers.

$$\lambda^{new}(t) = \lambda^{old}(t) - \varepsilon^{it}\frac{\partial(SWF)}{\partial(\lambda(t))} = \lambda^{old}(t) - \varepsilon^{it}(\sum_{i=1}^{n_{g1}} p_{g1}^{i}(t) + \sum_{j=1}^{n_{g2}} p_{g2}^{j}(t) - \sum_{k=1}^{n_{d1}} p_{d1}^{k}(t) - \sum_{l=1}^{n_{d2}} p_{d2}^{l}(t)) = \lambda^{old}(t) - \varepsilon^{it} * \Delta p(t) \quad (10)$$

$$p_{d1}^{k\,new}(t) = p_{d1}^{k\,old}(t) + \varepsilon^{it}\frac{\partial(SWF)}{\partial(p_{d1}^{k}(t))} = p_{d1}^{k\,old}(t) + \varepsilon^{it}\left(a_{d1}^{k} * p_{d1}^{k}(t) + b_{d1}^{k} - \lambda(t)\right) \quad (11)$$

$$p_{d2}^{k\,new}(t) = p_{d2}^{k\,old}(t) + \varepsilon^{it}\frac{\partial(SWF)}{\partial(p_{d2}^{k}(t))} = p_{d2}^{k\,old}(t) - \varepsilon^{it} * \lambda(t) \quad (12)$$

$$p_{g1}^{i\,new}(t) = p_{g1}^{i\,old}(t) + \varepsilon^{it}\frac{\partial(SWF)}{\partial\left(p_{g1}^{i}(t)\right)} = p_{g1}^{i\,old}(t) + \varepsilon^{it} * \left(\lambda(t) - \left(a_{g1}^{i} * p_{g1}^{i}(t) + b_{g1}^{i}\right)\right) \quad (13)$$

$$p_{g2}^{j\,new}(t) = p_{g2}^{j\,old}(t) + \varepsilon^{it}\frac{\partial(SWF)}{\partial\left(p_{g2}^{j}(t)\right)} = p_{g2}^{i\,old}(t) + \varepsilon^{it} * \lambda(t) \quad (14)$$

Equation (10) leads to the power balancing constraint. Also, optimal production and consumption of agents considering price stem from Eqs. (11) - (14). As can be seen, if the initial price is known for agents, they will compute the power difference and with updating that, the maximum welfare can be achieved in a decentralized manner. The decentralized power difference calculation is completely expressed in [52]. ε^{it} in above equations guarantees the algorithm convergence which is computed as follows. The convergence condition for this methodology which is based on the power difference calculation can be found in [13].

$$\varepsilon^{it} = 1000 * e^{-\left(\frac{it}{50}\right)} - \frac{1}{10} \tag{15}$$

3.5. Interaction of agents in the proposed EH

Having interactions, the agents can directly affect the settlement price and minimize their costs which leads to an increase in social welfare. The specifications of agents are as follows. The power updating for the electrical load agent for each scenario is according to (13) and

this agent is an FTOC. Also, it interrupts some loads by price changing and determines the interaction price based on cost function (5). Grid agent is the STOG and its power is calculated based on (14) to maximize social welfare. This agent buys the electricity offered by the PV agent and sells it to the absorption chiller. Also, the purchase price from EH is assumed to be 80% of its sale price. After the electricity price drops below the selling price to the grid, the grid agent reduces the sales capacity and proclaims another command, and the process continues when the interaction price exceeds the selling price.

The PV agent is an STOG and its power calculation is based on (14). The Eq. (16) converts solar irradiation to solar power where n_{panel} and $irr(t)$ are the number of panels and radiation intensity at time *t*, respectively. Also, η_{pv} and η_{inv} are the solar panel and the inverter efficiencies, respectively [34]. Therefore, first, the PV agent calculates its output based on Eq. (16).

$$p_{av}(t) = n_{panel} * A_{panel} * \eta_{pv} * \eta_{inv} * irr(t)\left(\frac{kw}{m^2}\right) \tag{16}$$

PV agent decreases its output power when the grid sale price is higher than the interaction price after computing the power difference and this recursive action will continue until the interaction price exceeds the grid sale price. Besides, the discharging of the PV agent during peak hours occurs through interaction with the grid agent. However, charging/discharging rates are restricted by battery capacity (x^{bat}) and their maximum rates. The charging and discharging rates of battery are based on (17) - (18). p_{ch}^{esMax} and p_{dis}^{esMax} are the maximum charging/discharging rates at time *t*. Also, $\eta_{ch}^{es}$and η_{dis}^{es} are charging and discharging efficiencies, respectively. p_{req}^{es} is the required power from the battery storage [40]. If this power is positive, the battery goes to a discharging state according to Eq. (17), otherwise, it goes to discharging state based on Eq. (18). Equation (19) represents the updating of state of the charge where $soc^{es}(t)$ is the state of charge at time *t* and $\alpha_{dis|ch}(t)$ is the binary variable that prevents the charging/discharging states at the same time. The electrical interaction process which includes PV agent, grid agent, electrical load agent, and MT agent is depicted in Fig. 2 [34].

$$p_{dis}^{es}(t) = \min(p_{dis}^{esMax}(t).(soc^{es}(t) - soc_{min}^{es}) * x^{bat} * \eta_{dis}^{es}.p_{req}^{es}) \tag{17}$$

$$p_{ch}^{es}(t) = \min(p_{ch}^{esMax}(t).\left(soc_{min}^{bat} - soc^{es}(t)\right) * \frac{x^{bat}}{\eta_{dis}^{es}}.p_{req}^{es}) \tag{18}$$

$$soc^{es}(t+1) = soc^{es}(t) + \frac{\alpha_{dis|ch}(t)*\eta_{ch}^{es}*p_{ch}^{es}(t)+\left(1-\alpha_{dis|ch}(t)\right)\left(\frac{p_{dis}^{es}(t)}{\eta_{dis}^{es}}\right)}{x^{bat}} \tag{19}$$

The MT agent takes part in both electrical and thermal interactions. First, it has an electrical interaction according to its production constraint (20). Then, the minimum heat production of this unit is calculated based on the electric generation in (21). k_h^{min} is a parameter that describes the percentage of electrical generation which leads to the thermal generation [34].

$$P_{mt_e}^{min} \leq P_{mt}^{e}(t) \leq P_{mt_e}^{max} \tag{20}$$

$$P_{mt_h}^{min}(t) = k_h^{min} * P_{mt}^{e}(t) \tag{21}$$

$$P_{mt_h}^{min}(t) \leq P_{mt}^{h}(t) \leq P_{mt_h}^{max} \tag{22}$$

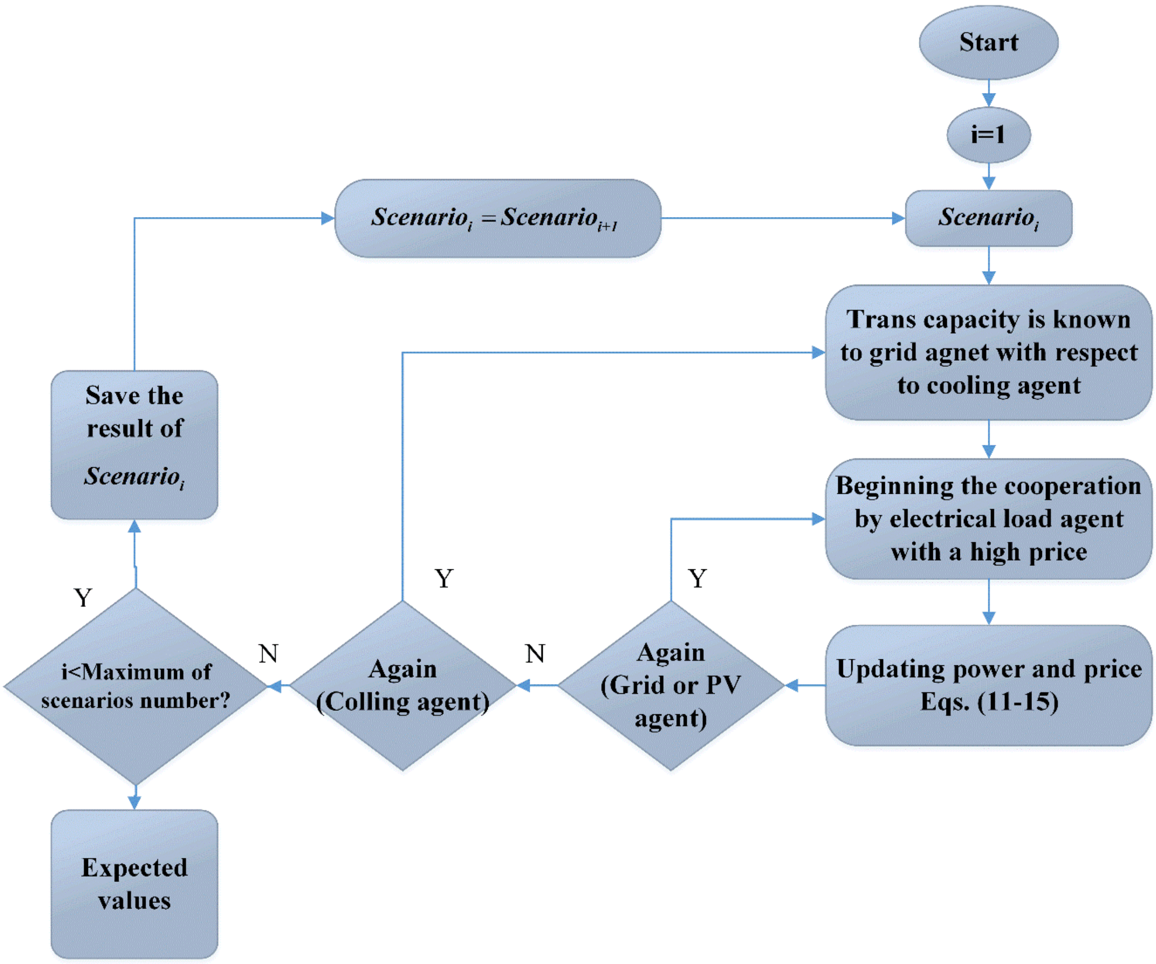

Fig. 2. Flowchart for electrical interaction

The boiler agent is also an FTOG and its power updates like the MT agent based on (13). The thermal load agent is an FTOC and updates its power due to (11). The cooling agent is a STOC that updates its power due to (12). The thermal interaction process which includes the cooling agent, thermal load agent, boiler agent, and MT agent is depicted in Fig. 3.

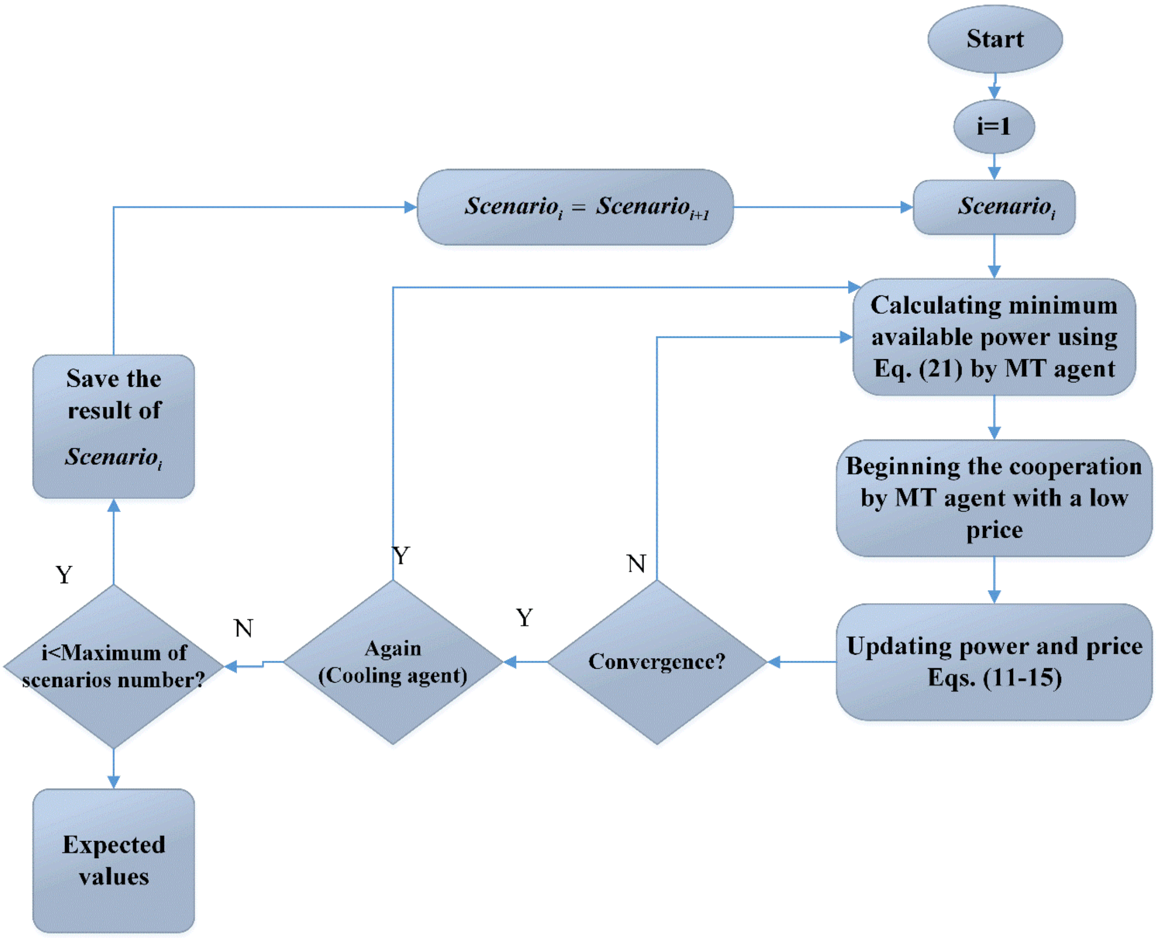

Fig. 3. Flowchart for thermal interaction

4. Stochastic scenarios

The agents face various uncertainty in all types of loads, PV generation, and upper grid prices. To deal with these uncertainties, the stochastic scenarios are employed. We use

Monte Carlo simulation and Kantorovich distance methods [51, 54] to generate a large number of scenarios and reduce them to more probable scenarios based on their distribution function. Each scenario includes information about hourly electrical load, thermal load, cooling load, electric, and gas prices. According to [55] Beta Probability Distribution Function (PDF) is the best distribution function to model the solar irradiance:

$$f_b(irr) = \begin{cases} \dfrac{\Gamma(\alpha+\beta)}{\Gamma(\alpha)\Gamma(\beta)} \times irr^{\alpha-1}(1-irr)^{\beta-1} & \text{for } 0 \le irr \le 1,\ \alpha \ge 0, \beta \ge 0 \\ 0 & \text{Otherwise} \end{cases} \tag{23}$$

Where *irr* is the solar irradiance (kW/m^2), α and β are Beta PDF parameters and $f_b(irr)$ is the Beta PDF of *irr*. The following equations are used to compute α and β using mean value μ and standard deviation σ of random variable *x* [55].

$$\alpha = \mu\left(\frac{\mu(1+\mu)}{\sigma^2} - 1\right) \tag{24}$$

$$\beta = (1-\mu)\left(\frac{\mu(1+\mu)}{\sigma^2} - 1\right) \tag{25}$$

We assume that the hourly forecasted data for types of load and prices are available for the agents. Also, we assume that the agents can fit the forecasting data into distributions using historical data [56-59]. For simplicity, the forecasting errors of electric and gas prices and also, electrical, thermal, and cooling loads are assumed to follow normal distributions with zero-mean and the standard deviations are 15% of their corresponding hourly values [60-63]. Moreover, we assume the uncertainties of the systems are independent. Based on the proposed PDFs, 500 scenarios for each parameter are generated by using the Monte Carlo simulation method. Then 50 more probable scenarios are selected by using fast-forward algorithm which minimize the Kantorovich distance as follows [64]:

$$D_K(Q,Q') = \sum_{s} \rho(s) \min_{s'} \left(\sum_{t=1}^{n_T} \left| y(s) - y(s') \right| \right) \tag{26}$$

Where Q and Q' are finite distribution of initial scenario s and reduced scenario s' respectively. $\rho(s)$ is also probability of scenario s and y is the uncertain parameter. The fast-forward algorithm is repetitive and in each iteration the scenario which minimize the Eq. (26) is selected. After reaching desired number of scenarios, the probabilities of selected scenarios are added [65]. Therefore, the output of the scenario reduction algorithm is a set of stochastic scenarios with their probabilities which are used in the proposed decentralized operating model. In other word, the proposed decentralized optimization is solved for each stochastic scenario and finally the expected values of optimal solutions are reported.

5. Stochastic decentralized operation model

In this section, the proposed formulations for decentralized operation in Eqs. (1) – (22) are re-written and will be solved for each stochastic scenario s with probability $\rho(s)$ as follows. Fig. 4 illustrate the whole stochastic decentralized operation.

$$C_{g1,s}(t) = \frac{1}{2} a_{g1} * p_{g1,s}(t)^2 + b_{g1} * p_{g1,s}(t) + c_{g1} \tag{27}$$

$$R_{g1,s}(t) = \lambda_s(t) * p_{g1,s}(t) \tag{28}$$

$$C_{g2,s}(t) = c_{g2} \tag{29}$$

$$R_{g2,s}(t) = \lambda_s(t) * p_{g2,s}(t) \tag{30}$$

$$R_{d1,s}(t) = \frac{1}{2} a_{d1} * p_{d1,s}(t)^2 + b_{d1} * p_{d1,s}(t) \tag{31}$$

$$C_{d1,s}(t) = \lambda_s(t) * p_{d1,s}(t) \tag{32}$$

$$C_{d2,s}(t) = \lambda_s(t) * p_{d2,s}(t) \tag{33}$$

$$ESWF = \sum_{s=1}^{ns}(\sum_{t=1}^{24}\Big(\sum_{i=1}^{n_{g1}}(R_{g1,s}^{i}(t) - C_{g1,s}^{i}(t)) + \sum_{j=1}^{n_{g2}}(R_{g2,s}^{j}(t) - C_{g2,s}^{j}(t)) +$$

$$\sum_{k=1}^{n_{d1}}(R_{d1,s}^{k}(t) - C_{d1,s}^{k}(t)) -$$

$$\sum_{l=1}^{n_{d2}} C_{d,s}^{l}(t)\Big)) \tag{34}$$

$$\lambda_s{}^{new}(t) = \lambda_s{}^{old}(t) - \varepsilon^{it}\frac{\partial(ESWF)}{\partial(\lambda_s(t))} = \lambda_s{}^{old}(t) - \varepsilon^{it}(\sum_{i=1}^{n_{g1}} p_{g1,s}^{i}(t) + \sum_{j=1}^{n_{g2}} p_{g2,s}^{j}(t) -$$

$$\sum_{k=1}^{n_{d1}} p_{d1,s}^{k}(t) - \sum_{l=1}^{n_{d2}} p_{d2,s}^{l}(t)) = \lambda_s{}^{old}(t) - \varepsilon^{it} * \Delta p_s(t) \tag{35}$$

$$p_{d1,s}^{k\,new}(t) = p_{d1,s}^{k\,old}(t) + \varepsilon^{it}\frac{\partial(ESWF)}{\partial(p_{d1,s}^{k}(t))} = p_{d1,s}^{k\,old}(t) + \varepsilon^{it}\left(a_{d1}^{k} * p_{d1,s}^{k}(t) + b_{d1}^{k} - \lambda_s(t)\right) \tag{36}$$

$$p_{d2,s}^{k\,new}(t) = p_{d2,s}^{k\,old}(t) + \varepsilon^{it}\frac{\partial(ESWF)}{\partial(p_{d2,s}^{k}(t))} = p_{d2,s}^{k\,old}(t) - \varepsilon^{it} * \lambda_s(t) \tag{37}$$

$$p_{g1,s}^{i\,new}(t) = p_{g1,s}^{i\,old}(t) + \varepsilon^{it}\frac{\partial(ESWF)}{\partial\left(p_{g1,s}^{i}(t)\right)} = p_{g1,s}^{i\,old}(t) + \varepsilon^{it} * \left(\lambda_s(t) - \left(a_{g1}^{i} * p_{g1,s}^{i}(t) + b_{g1}^{i}\right)\right) \tag{38}$$

$$p_{g2,s}^{j\,new}(t) = p_{g2,s}^{j\,old}(t) + \varepsilon^{it}\frac{\partial(ESWF)}{\partial\left(p_{g2,s}^{j}(t)\right)} = p_{g2,s}^{i\,old}(t) + \varepsilon^{it} * \lambda_s(t) \tag{39}$$

$$p_{av,s}(t) = n_{panel} * A_{panel} * \eta_{pv} * \eta_{inv} * irr_s(t) \tag{40}$$

$$p_{dis,s}^{es}(t) = \min(p_{dis}^{esMax}(t).(soc_s{}^{es}(t) - soc_{min}^{es}) * x^{bat} * \eta_{dis}^{es}.p_{req}^{es}) \tag{41}$$

$$p_{ch,s}^{es}(t) = \min(p_{ch}^{esMax}(t).\left(soc_{min}^{bat} - soc_s{}^{es}(t)\right) * \frac{x^{bat}}{\eta_{dis}^{es}}.p_{req}^{es}) \tag{42}$$

$$soc_s{}^{es}(t+1) = soc_s{}^{es}(t) + \frac{\alpha_{dis|ch}(t) * \eta_{ch}^{es} * p_{ch,s}^{es}(t) + \left(1 - \alpha_{dis|ch}(t)\right)\left(\frac{p_{dis,s}^{es}(t)}{\eta_{dis}^{es}}\right)}{x^{bat}} \tag{43}$$

$$P_{mt_e}^{min} \leq P_{mt,s}^{e}(t) \leq P_{mt_e}^{max} \tag{44}$$

$$P_{mt_{h,s}}^{min}(t) = k_h^{min} * P_{mt,s}^{e}(t) \tag{45}$$

$$P_{mt_h}^{min}(t) \leq P_{mt,s}^{h}(t) \leq P_{mt_h}^{max} \tag{46}$$

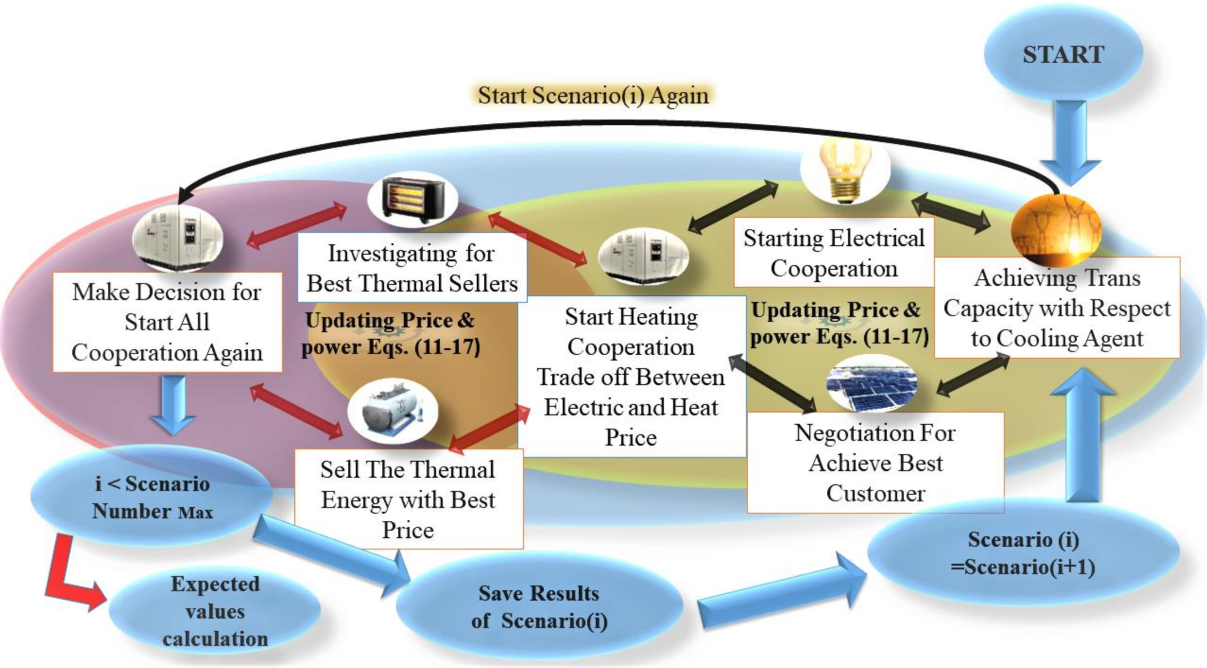

Fig. 4. Agents' interactions

6. Results and discussion

6.1. System data

To simulate the proposed stochastic process, the scenarios of solar irradiance, prices, loads of thermal, electrical, and cooling agents are generated based on their forecasted values from the University of Guilan [40]. These scenarios are plotted in Figs. 5-10. The capacity of existing equipment in this EH is provided in Table 2 [40]. The constant coefficients of entities that exist in both thermal and electrical interactions are taken from [66]. Also, the battery has a minimum and maximum charging/discharging rates of 25% and 10% of its total capacity with an efficiency of 90%, respectively. Moreover, the thermal storage has a minimum and maximum charging/discharging rates of 30% and 10% of its total capacity with an efficiency of 80%, respectively [67] . As the AnyLogic software has the required infrastructure for agent-based programming, in this regard, the simulation of this paper has been in java language due to providing a simple and user-friendly infrastructure for implementing the complex agent based communication.

Table 2. Size of EH's component

Cooling		**Grid**	**Boiler**	**Micro turbine**		**PV**	
Electrical Chiller [kW]	Thermal Chiller [kW]	Trans [kW]	Boiler [kW]	Thermal storage [kW]	Micro turbine [kW]	Battery [kWh]	PV [kW]
15	15	80	15	10	60	10	40

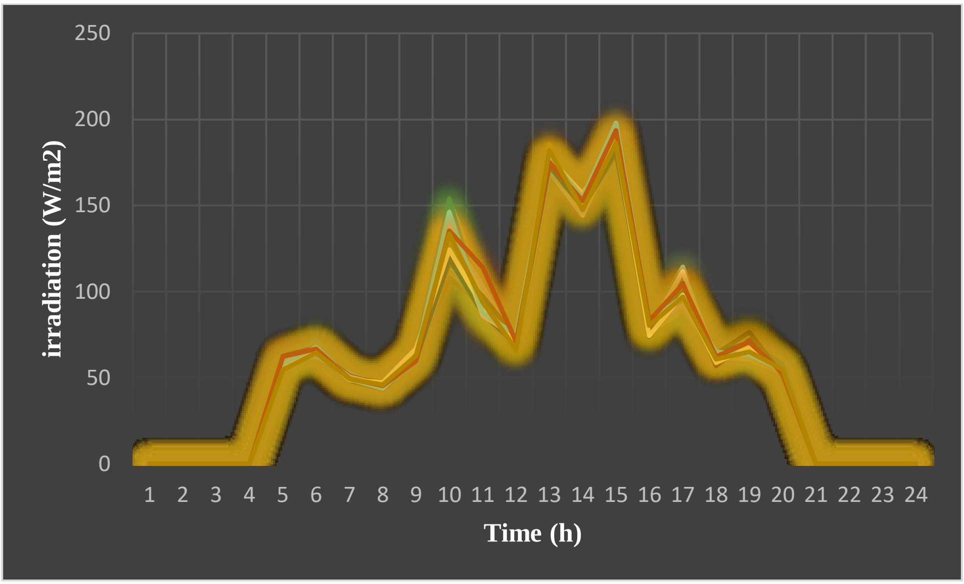

Fig. 5. Solar irradiance scenarios

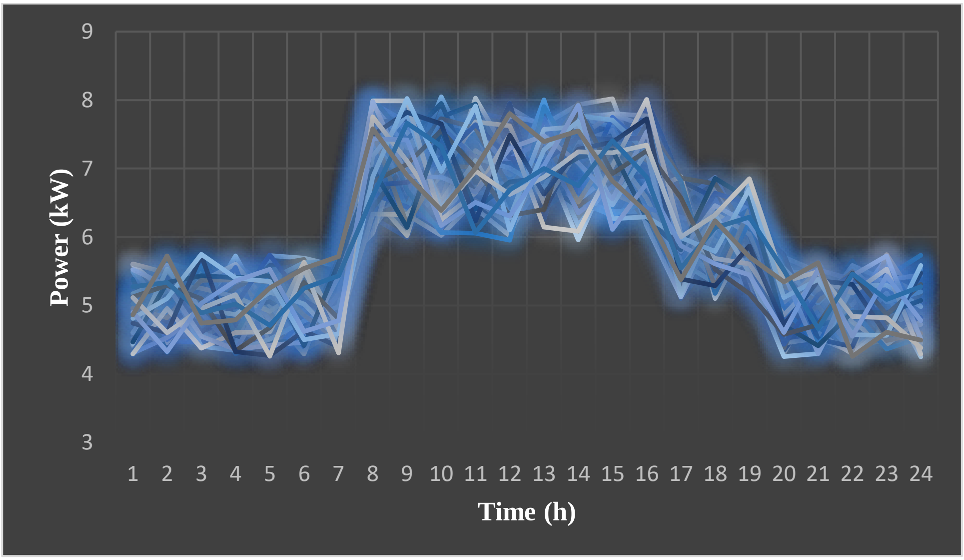

Fig. 6. Cooling power scenarios

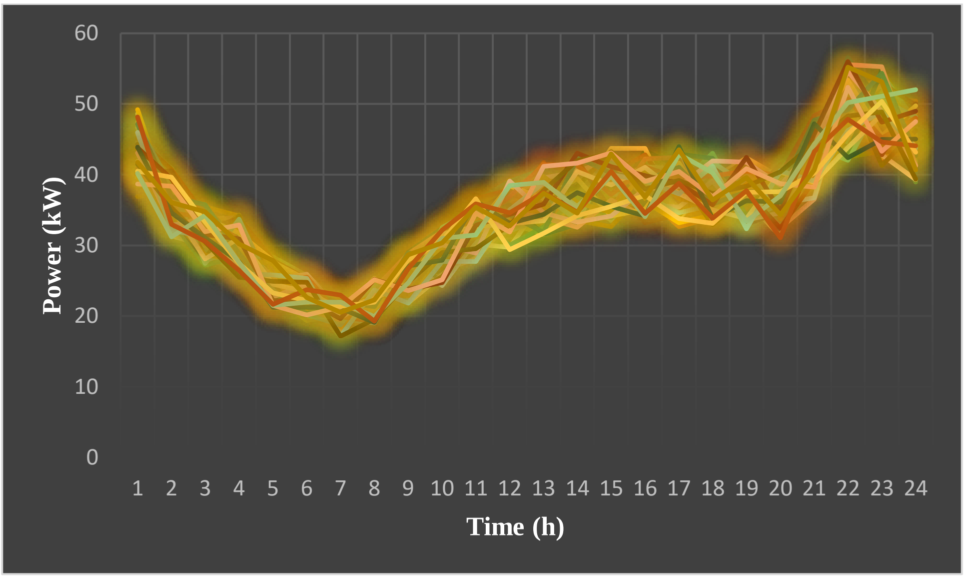

Fig. 7. Hourly upper bounds of electrical loads scenarios

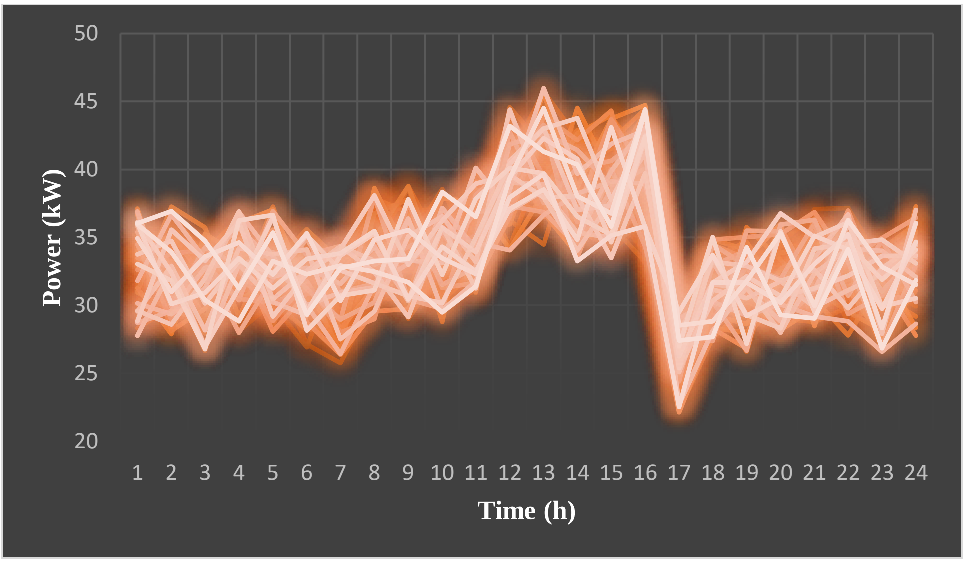

Fig. 8. Hourly upper bounds of thermal loads scenarios

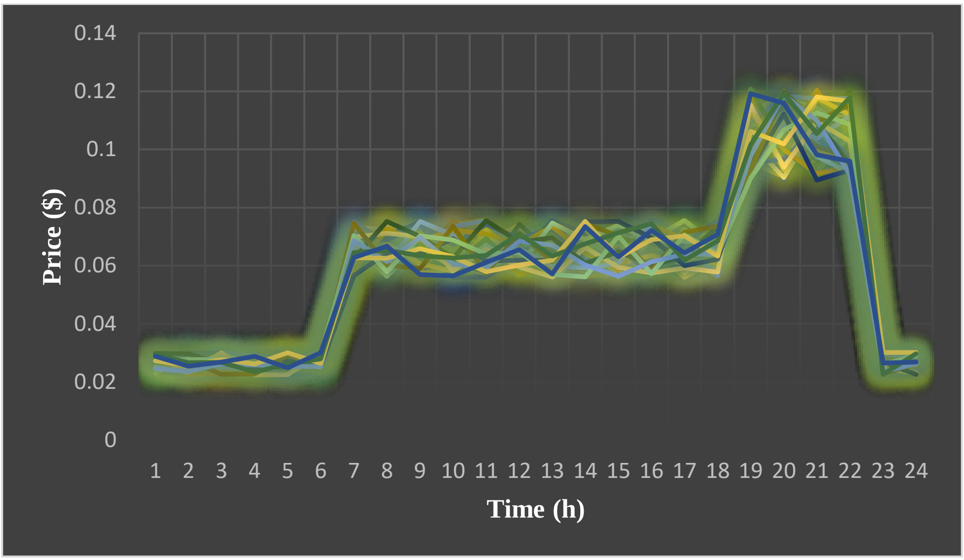

Fig. 9. Electric price scenarios

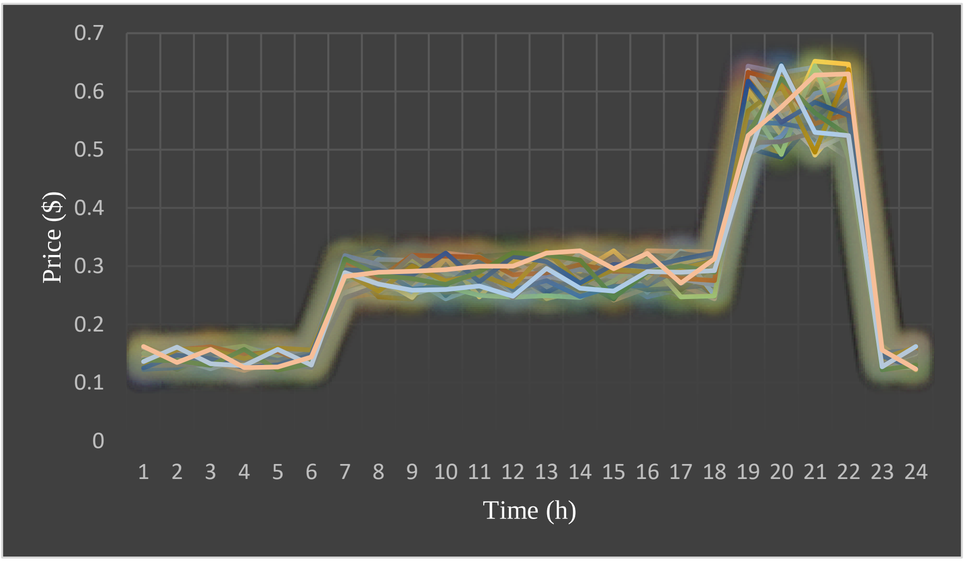

Fig. 10. Gas price scenarios

6.2. Simulation results of the proposed model

In this section, the behavior of the agents in the EH is explained for all scenarios so that the performance of the presented model becomes more transparent. As can be seen in Fig. 11, gas prices and grid sell prices have a direct impact on the price charged in the thermal (Heat Price) and electrical (Electric Price) interactions of the multi-energy system, respectively. Since gas price is higher than the grid sell price at all hours, the result of the price in thermal interaction is also higher than the price in electrical interaction. The direct effect of the gas price on the Heat Price is due to the direct dependence of the coefficients on the boiler agent and the thermal part of the MT agent. The reason why the price of electrical interaction is close to the grid sell price is explained below.

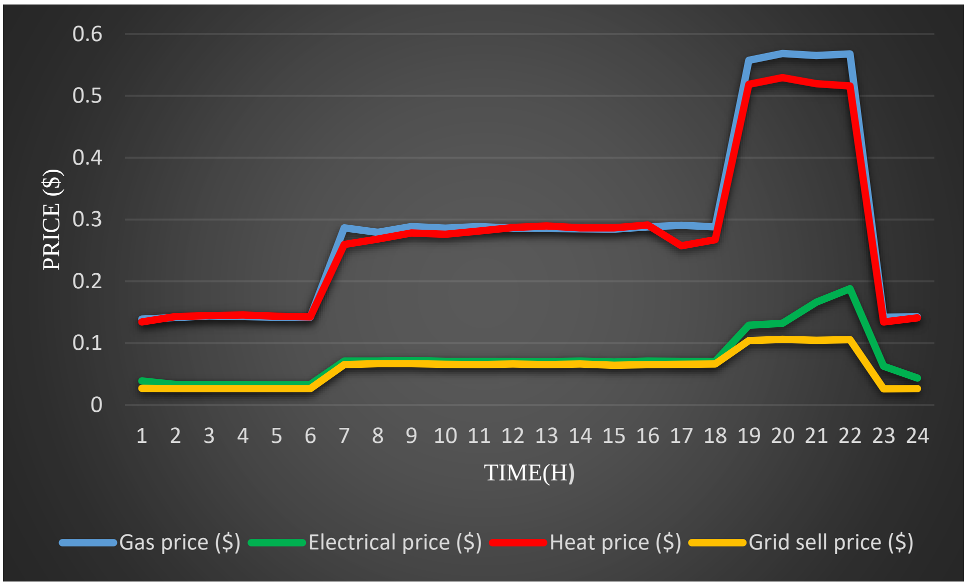

Fig.11. Expected thermal & electric clearing prices and expected electric and gas prices of upper grid

Fig. 12. shows that the cost of using solar energy is negligible, so it uses the maximum available energy during the day. But since this amount of solar energy is less than the electric charge at all hours of the day, so the upstream grid is most likely to determine the cost of thermal interaction for most hours, so the graph of the electrical interaction is similar to the upstream grid price graph. It should be noted that at peak hours of consumption since the amount of power consumed by the upstream grid doesn't cover the electrical

demand, so the EH compensates for its energy shortage through MT power generation. Hence, at the mentioned hour the electrical interaction clear price increases.

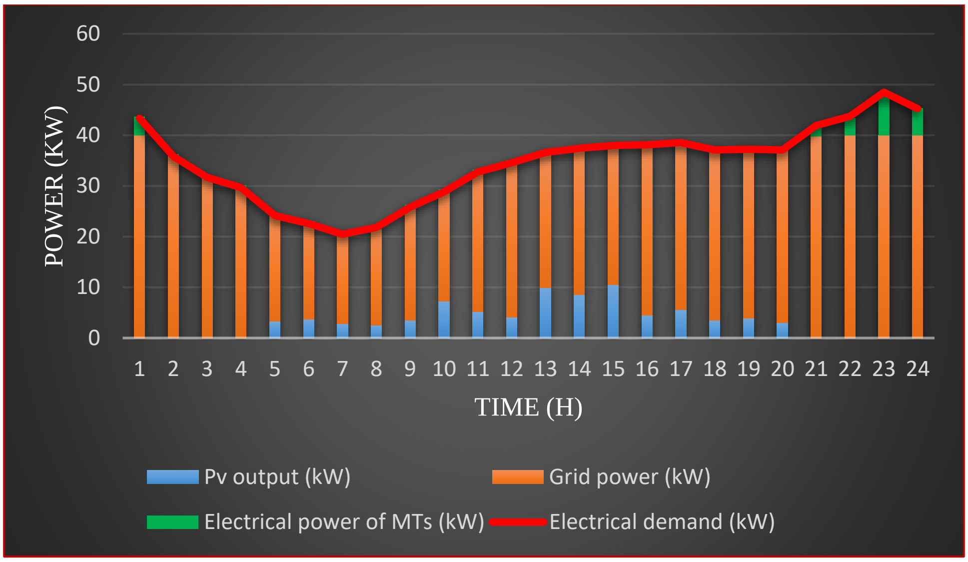

Fig. 12. Expected electrical power distributions result in electrical interaction

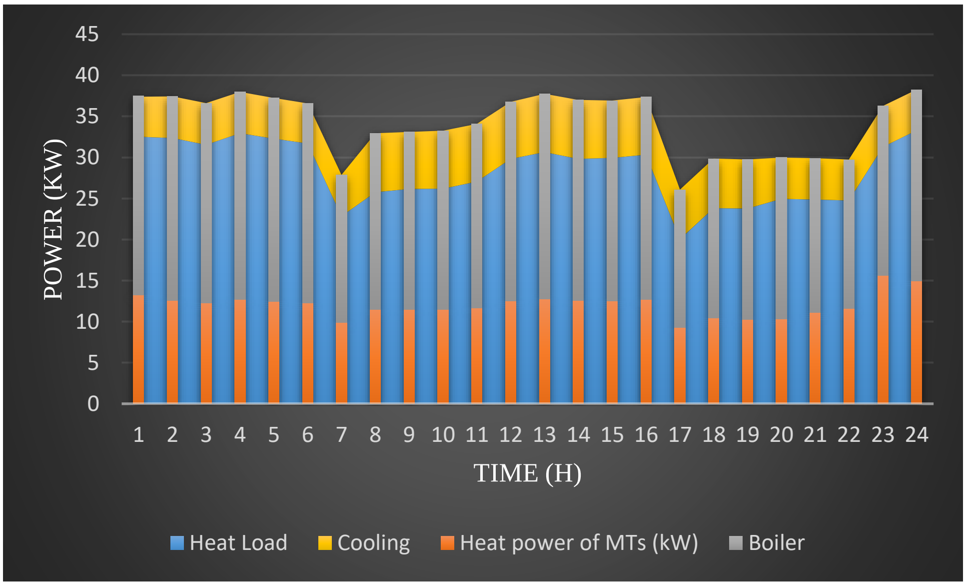

Fig. 13. Expected thermal power distribution results in thermal interaction

As can be seen from Fig. 13, most of the energy is supplied by the boiler during the day and compensates for the shortage of MT if needed. This is due to the higher coefficients in the thermal part of the MT agent than the boiler agent.

6.3. Comparison with deterministic and centralized models

In this section, the numerical results stemmed from the previous section are compared with deterministic and also with centralized models. It is worth mentioning that, the centralized optimization model is completely solved by CPLEX solver under GAMS [68] and is based on the written model in the appendix of [40]. In Table 3, it can be seen that in the decentralized state, considering the uncertainties in the input data, although the cost of MT, cooling and thermal load agent is higher than the deterministic model, the gain for the other agents makes the total benefit of the EH greater than the deterministic one. For example, the expected cost for MT agent is grown from 1503 $ in the deterministic model to 1636 $ in the stochastic one. However, the expected profit of the electrical load agent is increased from 6704 $ to 7223 $, and also the profit of the PV agent is slightly increased from 166 $ to 182 $ in the stochastic model. Therefore, considering the uncertainties of input data can change the optimal values. This is so important for the agent like PV which is a price maker and its interactions exert an influence on the clearing price.

On the other hand, as Table 3 illustrates, only the trend of PV agent is growing compared with its centralized model. This is because the PV agent fails to determine the selling/buying time slots on its own decisions in the centralized model, by the same token, the decentralized method makes the presence of PV agent more realistic and efficient. It should be noted that in the centralized state, due to the optimizer's access to all information, the net gain will be better than the decentralized state. As can be seen, the whole benefit in the centralized model is 7287 $ compared with 6252 $ in the stochastic decentralized one.

Table 3. Expected operating costs in different operation models

Operation Model	PV agent [$]	MT agent [$]	Grid agent [$]	Boiler agent [$]	Cooling agent [$]	Electrical load agent [$]	Thermal load agent [$]	Total [$]
Stochastic decentralized	-182	1636	-1726	-1583	1196	-7223	1630	-6252
deterministic decentralized	-162	1503	-1511	-1444	1008	-6704	1488	-5826
centralized	-63	1965	-1878	-1583	2120	-7856	7.5	-7287

6.4. Sensitivity analysis on the PV agent presence

The main influence of the size of the PV agent as an active participant is provided in Table 4 and compare with the base state 40 kW. As can be seen, by increasing the capacity of the PV agent, the participation of the upstream grid agent in the electrical interaction of the multi-energy system decreases, and as a result, the profit of this agent decreases as well. Since the cost of produced electricity with the PV agent is much cheaper than the grid agent production so the electric load agent can provide needed energy with much less cost which leads to the total cost reduction for this agent. The effect on the other elements is negligible.

Table 4. The effect of PV agent capacity on the cost of components

Size (kW) / Cost ($)	0	20	40	60	80
PV agent	0	-92	-182	-258	-340
Electrical load agent	-6284	-6572	-7223	-8161	-8378
Grid agent	-2295	-2002	-1726	-1467	-1294

6.5. The value of stochastic solution

A useful indicator that represents the effectiveness of stochastic optimization is the value of a stochastic solution (VSS). This indicator shows how much savings can be made by using stochastic scenarios instead of deterministic quantities. In other words, VSS represents the cost of ignoring the uncertainty in decision making. The smallness of the VSS shows that the solution of the deterministic method is an appropriate approximation of the actual solution of the problem.

$$VSS = z_{EV} - z_S \tag{47}$$

In (47), z_{EV} represents the value of objective function obtained from the deterministic method and z_S represents the value of objective function obtained from the stochastic method. Table 5 shows the results of this process. According to this table, by taking into account the stochastic scenarios of loads, solar irradiance, and prices, the expected cost is decreased by 7.3% (expected profit is increased by 7.3%).

Table 5 – VSS of system scenarios

z_{EV}	z_S	VSS
-5826	-6252	426 (7.3%)

7. Conclusion

In this paper, a stochastic decentralized operation model for an EH is proposed using MAS. Considering the uncertainty in input data, the cost of the agents is changed compared to their deterministic one. Therefore, the variation in the forecasting data can affect making decisions of agents and their profits. This model does not rely on a specific agent and if any interruption occurs, the system can be still operational. Therefore, the main results of this paper are:

- The stochastic decentralized operation of the system led to a higher total benefit due to considering its input data uncertainties. The VSS index showed an increase of 7.3% for the total gain.
- The whole social benefit in the decentralized model has decreased compared to its centralized one due to two main reasons. Firstly, the private ownership of some agents like the PV agent made its profit higher and this led to a drop in social benefit. Secondly, in a decentralized model, the agents fail to gather all information of the system and they just use the information arising from their interactions with other agents.
- The growth in the PV size can lead to higher profit for the whole system. This is because not only its own profit increase but also the electrical load agent can procure more affordable electricity from this agent.

In the future work, develop the model into a large scale system is suggested with different energy components like hydrogen storage system or etc.

Acknowledgement

This work is supported by the National Natural Science Foundation of China (61772454), and by a grant from the Programs of Transformation and Upgrading of Industries and Information Technologies of Jiangsu Province (No. JITC-1900AX2038/01).

References

[1] S. Boudoudouh and M. Maâroufi, "Multi agent system solution to microgrid implementation," *Sustainable Cities and Society,* vol. 39, pp. 252-261, 2018/05/01/ 2018, doi: https://doi.org/10.1016/j.scs.2018.02.020.

[2] N. Nasiri *et al.*, "A bi-level market-clearing for coordinated regional-local multi-carrier systems in presence of energy storage technologies," *Sustainable Cities and Society,* vol. 63, p. 102439, 2020/12/01/ 2020, doi: https://doi.org/10.1016/j.scs.2020.102439.

[3] S. Mohseni and S. M. Moghaddas-Tafreshi, "A multi-agent system for optimal sizing of a cooperative self-sustainable multi-carrier microgrid," *Sustainable Cities and Society,* vol. 38, pp. 452-465, 2018/04/01/ 2018, doi: https://doi.org/10.1016/j.scs.2018.01.016.

[4] N. M. Isa, C. W. Tan, and A. H. M. Yatim, "A comprehensive review of cogeneration system in a microgrid: A perspective from architecture and operating system," *Renewable and Sustainable Energy Reviews,* vol. 81, pp. 2236-2263, 2018/01/01/ 2018, doi: https://doi.org/10.1016/j.rser.2017.06.034.

[5] D. S. Setlhaolo, S Zhang, J, "Residential load management in an energy hub with heat pump water heater," *Applied Energy,* vol. 208, pp. 551 - 560, 2017.

[6] S. Cao, "Comparison of the energy and environmental impact by integrating a H2 vehicle and an electric vehicle into a zero-energy building," *Energy Conversion and Management,* vol. 123, pp. 153-173, 2016/09/01/ 2016, doi: https://doi.org/10.1016/j.enconman.2016.06.033.

[7] K. Siler-Evans, M. G. Morgan, and I. L. Azevedo, "Distributed cogeneration for commercial buildings: Can we make the economics work?," *Energy Policy,* vol. 42, pp. 580-590, 2012/03/01/ 2012, doi: https://doi.org/10.1016/j.enpol.2011.12.028.

[8] X. Xu, H. Jia, D. Wang, D. C. Yu, and H.-D. Chiang, "Hierarchical energy management system for multi-source multi-product microgrids," *Renewable Energy,* vol. 78, pp. 621-630, 2015/06/01/ 2015, doi: https://doi.org/10.1016/j.renene.2015.01.039.

[9] S. D. Beigvand, H. Abdi, and M. La Scala, "A general model for energy hub economic dispatch," *Applied Energy,* vol. 190, pp. 1090-1111, 2017/03/15/ 2017, doi: https://doi.org/10.1016/j.apenergy.2016.12.126.

[10] H. Lin, Y. Liu, Q. Sun, R. Xiong, H. Li, and R. Wennersten, "The impact of electric vehicle penetration and charging patterns on the management of energy hub – A multi-agent system simulation," *Applied Energy,* vol. 230, pp. 189-206, 2018/11/15/ 2018, doi: https://doi.org/10.1016/j.apenergy.2018.08.083.

[11] P. Bahramnia, S. M. Hosseini Rostami, J. Wang, and G.-j. Kim, "Modeling and Controlling of Temperature and Humidity in Building Heating, Ventilating, and Air Conditioning System Using Model Predictive Control," *Energies,* vol. 12, no. 24, p. 4805, 2019. [Online]. Available: https://www.mdpi.com/1996-1073/12/24/4805.

[12] J. Zhang, S. Zhong, T. Wang, H.-C. Chao, and J. Wang, "Blockchain-based Systems and Applications: A Survey," *2020,* vol. 21, no. 1, p. 14, 2020-01-01 2020. [Online]. Available: https://jit.ndhu.edu.tw/article/view/2217.

[13] W. Zhang, Y. Xu, W. Liu, C. Zang, and H. Yu, "Distributed Online Optimal Energy Management for Smart Grids," *IEEE Transactions on Industrial Informatics,* vol. 11, no. 3, pp. 717-727, 2015, doi: 10.1109/TII.2015.2426419.

[14] J. Wang, Y. Yang, T. Wang, R. S. Sherratt, and J. Zhang, "Big Data Service Architecture: A Survey," *2020,* vol. 21, no. 2, p. 13, 2020-03-01 2020. [Online]. Available: https://jit.ndhu.edu.tw/article/view/2261.

[15] A. Riahifard, S. M. Hosseini Rostami, J. Wang, and H.-J. Kim, "Adaptive Leader-Follower Formation Control of Under-actuated Surface Vessels with Model Uncertainties and Input Constraints," *Applied Sciences,* vol. 9, no. 18, p. 3901, 2019. [Online]. Available: https://www.mdpi.com/2076-3417/9/18/3901.

[16] S. M. H. Rostami, A. K. Sangaiah, J. Wang, and X. Liu, "Obstacle avoidance of mobile robots using modified artificial potential field algorithm," *EURASIP Journal on Wireless Communications and Networking,* vol. 2019, no. 1, p. 70, 2019/03/18 2019, doi: 10.1186/s13638-019-1396-2.

[17] A. K. Sangaiah, M. Sadeghilalimi, A. A. R. Hosseinabadi, and W. Zhang, "Energy Consumption in Point-Coverage Wireless Sensor Networks via Bat Algorithm," *IEEE Access,* vol. 7, pp. 180258-180269, 2019.

[18] A. K. Sangaiah, A. A. R. Hosseinabadi, M. B. Shareh, S. Y. Bozorgi Rad, A. Zolfagharian, and N. Chilamkurti, "IoT Resource Allocation and Optimization Based on Heuristic Algorithm," *Sensors,* vol. 20, no. 2, p. 539, 2020. [Online]. Available: https://www.mdpi.com/1424-8220/20/2/539.

[19] A. Soroudi and T. Amraee, "Decision making under uncertainty in energy systems: State of the art," *Renewable and Sustainable Energy Reviews,* vol. 28, pp. 376-384, 2013/12/01/ 2013, doi: https://doi.org/10.1016/j.rser.2013.08.039.

[20] S. D. J. McArthur *et al.*, "Multi-Agent Systems for Power Engineering Applications—Part I: Concepts, Approaches, and Technical Challenges," *IEEE Transactions on Power Systems,* vol. 22, no. 4, pp. 1743-1752, 2007, doi: 10.1109/TPWRS.2007.908471.

[21] S. Tian and S. Chang, "An agent-based model of household energy consumption," *Journal of Cleaner Production,* vol. 242, p. 118378, 2020/01/01/ 2020, doi: https://doi.org/10.1016/j.jclepro.2019.118378.

[22] J. Yu, C. Dou, and X. Li, "MAS-Based Energy Management Strategies for a Hybrid Energy Generation System," *IEEE Transactions on Industrial Electronics,* vol. 63, no. 6, pp. 3756-3764, 2016, doi: 10.1109/TIE.2016.2524411.

[23] C. Dou, D. Yue, X. Li, and Y. Xue, "MAS-Based Management and Control Strategies for Integrated Hybrid Energy System," *IEEE Transactions on Industrial Informatics,* vol. 12, no. 4, pp. 1332-1349, 2016, doi: 10.1109/TII.2016.2569506.

[24] C.-x. Dou and B. Liu, "Hierarchical management and control based on MAS for distribution grid via intelligent mode switching," *International Journal of Electrical Power & Energy Systems,* vol. 54, pp. 352-366, 2014/01/01/ 2014, doi: https://doi.org/10.1016/j.ijepes.2013.07.029.

[25] T. Yue, R. Long, H. Chen, J. Liu, H. Liu, and Y. Gu, "Energy-saving behavior of urban residents in China: A multi-agent simulation," *Journal of Cleaner Production,* vol. 252, p. 119623, 2020/04/10/ 2020, doi: https://doi.org/10.1016/j.jclepro.2019.119623.

[26] M. W. Khan, J. Wang, M. Ma, L. Xiong, P. Li, and F. Wu, "Optimal energy management and control aspects of distributed microgrid using multi-agent systems," *Sustainable Cities and Society,* vol. 44, pp. 855-870, 2019/01/01/ 2019, doi: https://doi.org/10.1016/j.scs.2018.11.009.

[27] S. M. H. Rostami, A. K. Sangaiah, J. Wang, and H.-j. Kim, "Real-time obstacle avoidance of mobile robots using state-dependent Riccati equation approach," *EURASIP Journal on Image and Video Processing,* vol. 2018, no. 1, p. 79, 2018/08/29 2018, doi: 10.1186/s13640-018-0319-1.

[28] A. Anvari-Moghaddam, A. Rahimi-Kian, M. S. Mirian, and J. M. Guerrero, "A multi-agent based energy management solution for integrated buildings and microgrid system," *Applied Energy,* vol. 203, pp. 41-56, 2017/10/01/ 2017, doi: https://doi.org/10.1016/j.apenergy.2017.06.007.

[29] F. Kamyab and S. Bahrami, "Efficient operation of energy hubs in time-of-use and dynamic pricing electricity markets," *Energy,* vol. 106, pp. 343-355, 2016/07/01/ 2016, doi: https://doi.org/10.1016/j.energy.2016.03.074.

[30] S. Skarvelis-Kazakos, P. Papadopoulos, I. Grau Unda, T. Gorman, A. Belaidi, and S. Zigan, "Multiple energy carrier optimisation with intelligent agents," *Applied Energy,* vol. 167, pp. 323-335, 2016/04/01/ 2016, doi: https://doi.org/10.1016/j.apenergy.2015.10.130.

[31] F. Z. Harmouch, N. Krami, and N. Hmina, "A multiagent based decentralized energy management system for power exchange minimization in microgrid cluster," *Sustainable Cities and Society,* vol. 40, pp. 416-427, 2018/07/01/ 2018, doi: https://doi.org/10.1016/j.scs.2018.04.001.

[32] E. Samadi, A. Badri, and R. Ebrahimpour, "Decentralized multi-agent based energy management of microgrid using reinforcement learning," *International Journal of Electrical Power & Energy Systems,* vol. 122, p. 106211, 2020/11/01/ 2020, doi: https://doi.org/10.1016/j.ijepes.2020.106211.

[33] M. Mohiti, H. Monsef, A. Anvari-moghaddam, J. Guerrero, and H. Lesani, "A decentralized robust model for optimal operation of distribution companies with private microgrids," *International Journal of Electrical Power & Energy Systems,* vol. 106, pp. 105-123, 2019/03/01/ 2019, doi: https://doi.org/10.1016/j.ijepes.2018.09.031.

[34] A. Sheikhi, M. Rayati, S. Bahrami, A. M. Ranjbar, and S. Sattari, "A cloud computing framework on demand side management game in smart energy hubs," *International Journal of Electrical Power & Energy Systems,* vol. 64, pp. 1007-1016, 2015/01/01/ 2015, doi: https://doi.org/10.1016/j.ijepes.2014.08.020.

[35] N. Cai, N. Nguyen Thi Thanh, and J. Mitra, "Economic dispatch in microgrids using multi-agent system," in *2012 North American Power Symposium (NAPS)*, 9-11 Sept. 2012 2012, pp. 1-5, doi: 10.1109/NAPS.2012.6336435.

[36] R. Olfati-Saber, J. A. Fax, and R. M. Murray, "Consensus and Cooperation in Networked Multi-Agent Systems," *Proceedings of the IEEE,* vol. 95, no. 1, pp. 215-233, 2007, doi: 10.1109/JPROC.2006.887293.

[37] Y.-S. Li, H.-G. Zhang, B.-N. Huang, and F. Teng, "Distributed Optimal Economic Dispatch Based on Multi-Agent System Framework in Combined Heat and Power Systems," *Applied Sciences,* vol. 6, no. 10, p. 308, 2016. [Online]. Available: http://www.mdpi.com/2076-3417/6/10/308.

[38] S. Bahrami, M. Toulabi, S. Ranjbar, M. Moeini-Aghtaie, and A. M. Ranjbar, "A Decentralized Energy Management Framework for Energy Hubs in Dynamic Pricing Markets," *IEEE Transactions on Smart Grid,* vol. 9, no. 6, pp. 6780-6792, 2018, doi: 10.1109/TSG.2017.2723023.

[39] E. Kuznetsova, C. Ruiz, Y.-F. Li, and E. Zio, "Analysis of robust optimization for decentralized microgrid energy management under uncertainty," *International Journal of Electrical Power & Energy Systems,* vol. 64, pp. 815-832, 2015/01/01/ 2015, doi: https://doi.org/10.1016/j.ijepes.2014.07.064.

[40] A. M. Alishavandi and S. M. Moghaddas-Tafreshi, "Interactive decentralized operation with effective presence of renewable energies using multi-agent systems," *International Journal of Electrical Power & Energy Systems,* vol. 112, pp. 36-48, 2019/11/01/ 2019, doi: https://doi.org/10.1016/j.ijepes.2019.04.023.

[41] M. J. Shabani and S. M. Moghaddas-Tafreshi, "Fully-decentralized coordination for simultaneous hydrogen, power, and heat interaction in a multi-carrier-energy system considering private ownership," *Electric Power Systems Research,* vol. 180, p. 106099, 2020/03/01/ 2020, doi: https://doi.org/10.1016/j.epsr.2019.106099.

[42] H. Gao, S. Xu, Y. Liu, L. Wang, Y. Xiang, and J. Liu, "Decentralized optimal operation model for cooperative microgrids considering renewable energy uncertainties," *Applied Energy,* vol. 262, p. 114579, 2020/03/15/ 2020, doi: https://doi.org/10.1016/j.apenergy.2020.114579.

[43] A. Najafi, H. Falaghi, J. Contreras, and M. Ramezani, "Medium-term energy hub management subject to electricity price and wind uncertainty," *Applied Energy,* vol. 168, pp. 418-433, 2016/04/15/ 2016, doi: https://doi.org/10.1016/j.apenergy.2016.01.074.

[44] Y. Chen, W. Wei, F. Liu, Q. Wu, and S. Mei, "Analyzing and validating the economic efficiency of managing a cluster of energy hubs in multi-carrier energy systems," *Applied Energy,* vol. 230, pp. 403-416, 2018/11/15/ 2018, doi: https://doi.org/10.1016/j.apenergy.2018.08.112.

[45] A. Parisio, C. Del Vecchio, and A. Vaccaro, "A robust optimization approach to energy hub management," *International Journal of Electrical Power & Energy Systems,* vol. 42, no. 1, pp. 98-104, 2012/11/01/ 2012, doi: https://doi.org/10.1016/j.ijepes.2012.03.015.

[46] S. K. Mahdi Zarif, Mohammad Hossein Javidi, "Assessment of electricity price uncertainty impact on the operation of multi-carrier energy systems

" *IET Generation, Transmission & Distribution,* vol. 9, pp. 2586-2592, 2015.

[47] M. Shamshirband, J. Salehi, and F. S. Gazijahani, "Decentralized trading of plug-in electric vehicle aggregation agents for optimal energy management of smart renewable penetrated microgrids with the aim of CO2 emission reduction," *Journal of Cleaner Production,* vol. 200, pp. 622-640, 2018/11/01/ 2018, doi: https://doi.org/10.1016/j.jclepro.2018.07.315.

[48] H. Chamandoust, G. Derakhshan, and S. Bahramara, "Multi-objective performance of smart hybrid energy system with Multi-optimal participation of customers in day-ahead energy market," *Energy and Buildings,* vol. 216, p. 109964, 2020/06/01/ 2020, doi: https://doi.org/10.1016/j.enbuild.2020.109964.

[49] A. Mansour-Saatloo, M. A. Mirzaei, B. Mohammadi-Ivatloo, and K. Zare, "A Risk-Averse Hybrid Approach for Optimal Participation of Power-to-Hydrogen Technology-Based Multi-Energy Microgrid in Multi-Energy Markets," *Sustainable Cities and Society,* vol. 63, p. 102421, 2020/12/01/ 2020, doi: https://doi.org/10.1016/j.scs.2020.102421.

[50] P. Han, J. Wang, Y. Li, and Y. Han, "Hierarchical Agent-Based Integrated Modelling Approach for Microgrids with Adoption of EVs and HRES," *Journal of Applied Mathematics,* vol. 2014, p. 10, 2014, Art no. 808549, doi: 10.1155/2014/808549.

[51] H. H. N. Growe-kuska, and W. Romisch, "Scenario reduction and scenario tree construction for power management problems," *Power Management Problems, IEEE Bologna Power Tech Proceedings,* 2033.

[52] Y. Ma, W. Zhang, W. Liu, and Q. Yang, "Fully Distributed Social Welfare Optimization With Line Flow Constraint Consideration," *IEEE Transactions on Industrial Informatics,* vol. 11, no. 6, pp. 1532-1541, 2015.

[53] D. P. Bertsekas, *Nonlinear programming*. Athena Scientific, 1995.

[54] J. Wang, M. Shahidehpour, and Z. Li, "Security-Constrained Unit Commitment With Volatile Wind Power Generation," *IEEE Transactions on Power Systems,* vol. 23, no. 3, pp. 1319-1327, 2008, doi: 10.1109/TPWRS.2008.926719.

[55] Y. M. Atwa, E. F. El-Saadany, M. M. A. Salama, and R. Seethapathy, "Optimal Renewable Resources Mix for Distribution System Energy Loss Minimization," *IEEE Transactions on Power Systems,* vol. 25, no. 1, pp. 360-370, 2010, doi: 10.1109/TPWRS.2009.2030276.

[56] M. J. Salehpour and S. M. Moghaddas Tafreshi, "The effect of price responsive loads uncertainty on the risk-constrained optimal operation of a smart micro-grid," *International Journal of Electrical Power & Energy Systems,* vol. 106, pp. 546-560, 2019/03/01/ 2019, doi: https://doi.org/10.1016/j.ijepes.2018.10.027.

[57] B. Rasouli, J. M. Salehpour, J. Wang, and G.-j. Kim, "Optimal Day-Ahead Scheduling of a Smart Micro-Grid via a Probabilistic Model for Considering the Uncertainty of Electric Vehicles' Load," *Applied Sciences,* vol. 9, no. 22, 2019, doi: 10.3390/app9224872.

[58] M. J. Salehpour, H. Radmanesh, S. M. Hosseini Rostami, J. Wang, and H.-J. Kim, "Effect of Load Priority Modeling on the Size of Fuel Cell as an Emergency Power Unit in a More-Electric Aircraft," *Applied Sciences,* vol. 9, no. 16, p. 3241, 2019. [Online]. Available: https://www.mdpi.com/2076-3417/9/16/3241.

[59] M. J. Salehpour, O. Zarenia, S. M. Hosseini Rostami, J. Wang, and S.-J. Lim, "Convex multi-objective optimization for a hybrid fuel cell power system of more electric aircraft," *International Transactions on Electrical Energy Systems,* vol. 30, no. 7, p. e12427, 2020, doi: 10.1002/2050-7038.12427.

[60] D. T. Nguyen and L. B. Le, "Risk-Constrained Profit Maximization for Microgrid Aggregators With Demand Response," *IEEE Transactions on Smart Grid,* vol. 6, no. 1, pp. 135-146, 2015, doi: 10.1109/TSG.2014.2346024.

[61] C. Sahin, M. Shahidehpour, and I. Erkmen, "Allocation of Hourly Reserve Versus Demand Response for Security-Constrained Scheduling of Stochastic Wind Energy," *IEEE Transactions on Sustainable Energy,* vol. 4, no. 1, pp. 219-228, 2013, doi: 10.1109/TSTE.2012.2213849.

[62] Z. Chen, L. Wu, and Y. Fu, "Real-Time Price-Based Demand Response Management for Residential Appliances via Stochastic Optimization and Robust Optimization," *IEEE Transactions on Smart Grid,* vol. 3, no. 4, pp. 1822-1831, 2012, doi: 10.1109/TSG.2012.2212729.

[63] D. Zhang, N. Shah, and L. G. Papageorgiou, "Efficient energy consumption and operation management in a smart building with microgrid," *Energy Conversion and Management,* vol. 74, no. Supplement C, pp. 209-222, 2013/10/01/ 2013, doi: https://doi.org/10.1016/j.enconman.2013.04.038.

[64] S. M. M. t. Mohammad Javad Salehpour, "A TWO-STAGE STOCHASTIC OPTIMIZATION BASED-ON MONTE CARLO SIMULATION FOR MAXIMIZING THE PROFITABILITY OF A SMART MICROGRID," *Journal of Hyperstructures,* 2018.

[65] M. Carrion, A. B. Philpott, A. J. Conejo, and J. M. Arroyo, "A Stochastic Programming Approach to Electric Energy Procurement for Large Consumers," *IEEE Transactions on Power Systems,* vol. 22, no. 2, pp. 744-754, 2007.

[66] I. Gerami Moghaddam, M. Saniei, and E. Mashhour, "Improvement of energy performance employing electrical heat pump in scheduling a residential energy hub," vol. 26, no. 12, pp. 2618-2642, 2016, doi: doi:10.1002/etep.2224.

[67] "E-storage: Shifting from cost to value Wind and solar applications." www.worldenergy.org (accessed.

[68] M. J. Salehpour and S. M. M. Tafreshi, "Contract-based utilization of plug-in electric vehicle batteries for day-ahead optimal operation of a smart micro-grid," *Journal of Energy Storage,* vol. 27, p. 101157, 2020/02/01/ 2020, doi: https://doi.org/10.1016/j.est.2019.101157.